

Effects of Consolidation under a Penetrating Footing in Carbonate Silty Clay

Britta Bienen¹; Raffaele Ragni²; Mark J. Cassidy³; and Samuel A. Stanier⁴

Abstract: The effects of consolidation under a footing are generally viewed as beneficial due to the resulting increased capacity. Consolidation may also be actively sought because it minimizes footing embedment, which can be critical for the installation of mobile offshore jack-ups because available leg length is limited. However, it can also set the platform footing up to subsequently punch through the strengthened zone, with potentially serious consequences. The problem is complex due to the three-dimensional nature of consolidation. Further, footing penetration leaves the soil above heavily remolded and generates large excess pore pressures below, such that the soil state even prior to consolidation is significantly altered from its in situ conditions. This study has taken an experimental approach to investigate the effects of consolidation around a footing penetrating into carbonate silty clay and, following detailed discussion of the response, offers a framework to predict the changes to the load-penetration curve. DOI: [10.1061/\(ASCE\)GT.1943-5606.0001339](https://doi.org/10.1061/(ASCE)GT.1943-5606.0001339). © 2015 American Society of Civil Engineers.

Author keywords: Consolidation; Bearing capacity; Offshore engineering; Punch through; Jack-up platform; Footing penetration; Particle image velocimetry (PIV); Carbonate; Silt.

Introduction

Mobile offshore jack-up drilling rigs are relocated frequently, spending as little as weeks or even days at any one site. At every location, the spudcan footings are penetrated into the seabed until the target bearing capacity is met to support the jack-up. This typically exceeds the self-weight of the platform, with additional preload provided in the form of seawater pumped into ballast tanks, to provide a safety margin against storm loading. Accident reports (Osborne et al. 2006; Hunt 2008; Jack et al. 2013) alert to the fact that the majority of failures remain related to geotechnical issues, with punch-through (uncontrolled rapid leg penetration) the leading cause. Punch through is a common risk in layered strata with significant strength differences that may result in extensive damage to the platform. This area has therefore received considerable research attention recently with investigation of both sand overlying clay (Craig and Chua 1990; Teh et al. 2010; Qiu and Grabe

2012; Yu et al. 2012; Lee et al. 2013a, b; Hu et al. 2014) and clay stratification of various strength ratios (Hossain and Randolph 2010a, b).

Punch-through potential, however, can also be man-made [International Organization for Standardization (ISO) 2012] "as a result of soil consolidation occurring during pauses in leg penetration whilst the spudcan is loaded to less than full preload. Such pauses can occur during installation operations or geotechnical investigation from a jack-up prior to full preloading." These pauses allow dissipation of excess pore pressures generated during the preceding loading event and hence increase the effective stresses in the soil. However, the effect will be localized such that additional loading, for instance on recommencement of preloading, may lead to the spudcan punching through this strengthened zone. Even relatively short pauses, such as preload holding times of approximately 3–4 h, have been reported to have contributed to subsequent punch-through failure in the field (Brennan et al. 2006).

The effect of pauses in spudcan penetration and the ensuing consolidation on the subsequent response was investigated experimentally by Bienen and Cassidy (2013) following two preliminary tests with the same apparatus by Barbosa-Cruz (2007). Importantly, these experiments were performed in a geotechnical centrifuge such that stress levels are similar to the prototype situation (Gaudin et al. 2011b). As a result, soil failure mechanisms in the model test are expected to be representative of those in the field, with quantities such as loads and displacements related via established scaling laws (Garnier et al. 2007). In the centrifuge experiments, penetration resistance was found to be enhanced postconsolidation, as expected. The peak resistance as well as the extent of the zone of soil strengthened by the consolidation was demonstrated to depend on the length of the period of consolidation, which is also expected. Punch-through risk, however, is not only determined by the magnitude of peak resistance, but crucially the response following the peak. The gradient of resistance reduction postpeak was identified to be related to the length of the consolidation period and importantly to the load (or pressure) on the spudcan during the pause in penetration. Fig. 1 illustrates schematically the effect of consolidation on the load-penetration curve of a spudcan footing.

¹Senior Lecturer, ARC Postdoctoral Fellow, Centre for Offshore Foundation Systems and ARC CoE for Geotechnical Science and Engineering, Univ. of Western Australia, 35 Stirling Hwy Crawley, Perth, WA 6009, Australia (corresponding author). E-mail: britta.bienen@uwa.edu.au

²Ph.D. Candidate, Centre for Offshore Foundation Systems and ARC CoE for Geotechnical Science and Engineering, Univ. of Western Australia, 35 Stirling Hwy Crawley, Perth, WA 6009, Australia. E-mail: 21358454@student.uwa.edu.au

³Winthrop Professor, ARC Laureate Fellow, Centre for Offshore Foundation Systems and ARC CoE for Geotechnical Science and Engineering, Univ. of Western Australia, 35 Stirling Hwy Crawley, Perth, WA 6009, Australia. E-mail: mark.cassidy@uwa.edu.au

⁴Research Associate, Centre for Offshore Foundation Systems and ARC CoE for Geotechnical Science and Engineering, Univ. of Western Australia, 35 Stirling Hwy Crawley, Perth, WA 6009, Australia. E-mail: sam.stanier@uwa.edu.au

Note. This manuscript was submitted on May 27, 2014; approved on March 24, 2015; published online on May 12, 2015. Discussion period open until October 12, 2015; separate discussions must be submitted for individual papers. This paper is part of the *Journal of Geotechnical and Geoenvironmental Engineering*, © ASCE, ISSN 1090-0241/04015040(\$25.00).

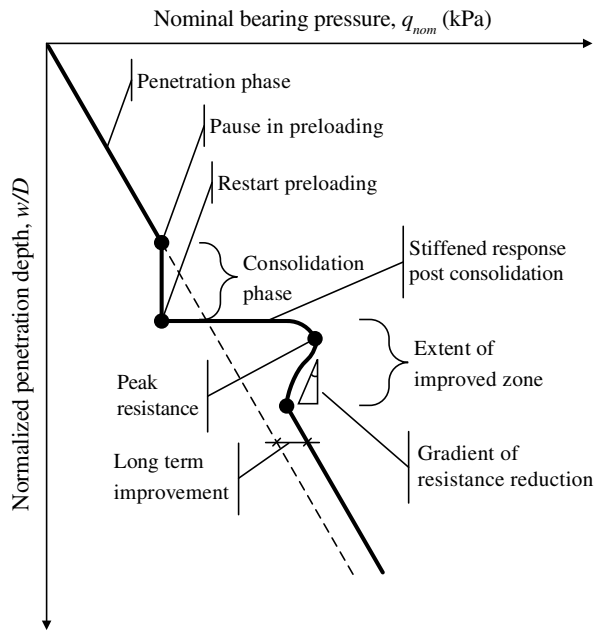


Fig. 1. Effect of consolidation on the load-penetration curve of a footing

Kaolin clay was chosen in these first series of experiments because of its well-known characteristics because it has been used in centrifuge testing at the University of Western Australia for more than two decades. Importantly, the coefficient of consolidation of kaolin clay allows investigation of a range of degrees of consolidation under a penetrating model footing in the centrifuge that represents a large-diameter spudcan in the field. The results were presented in nondimensional form. In particular, the increase in peak bearing capacity, the extent of the improved zone, and the severity of postpeak capacity reduction were provided as design charts relating to the nondimensional time of consolidation, $T = c_v t / D^2$, where c_v is the coefficient of consolidation, t is the consolidation time, and D is the foundation diameter. This representation was chosen as on the premise of similar soil characteristics, the findings may be viewed as indicative of the response of more permeable soils in the field.

For the range of likely pause durations during in-field jack-up installation (of the order of several hours to approximately 14 days

if consolidation is actively sought to minimize penetration depth), the effects of consolidation are expected to influence spudcan behavior in silty soils. Seabed soils offshore Australia often have a high calcium carbonate content, which adds significant challenge to jack-up installation (Erbrich 2005) due to high compressibility and sensitivity to grain crushing, which manifests itself in significant cyclic degradability.

This study therefore investigates the effects of consolidation under a penetrating footing in carbonate silty clay through experimentation in a geotechnical centrifuge. Similarities and differences in behavior compared with kaolin clay are discussed in detail before design charts are presented that capture the effect of consolidation on the subsequent response of a penetrating footing.

Experimental Setup and Procedure

Two series of experimental results are drawn on to investigate the problem in detail, the first being model tests with a full spudcan footing in the beam centrifuge (Randolph et al. 1991) and the second tests of a half spudcan model against a Perspex window in the drum centrifuge (Stewart et al. 1998) with a setup that allows particle image velocimetry (PIV) analysis to be performed. The soil sample preparation, testing procedure for both series, and experimental setup for the full spudcan tests is described in the following. For detailed information specific to the PIV setup used in the University of Western Australia drum centrifuge and relevant analysis techniques the reader is referred to Stanier and White (2013), while Stanier et al. (2014) provide details of PIV tests on kaolin clay similar to the carbonate silty clay tests discussed here. All tests were performed at 200g.

Footing Model and Instrumentation

The model spudcan was the same as used by Zhang et al. (2013, 2014). The spudcan was 60 mm in diameter at its widest section, which is equivalent to 12 m at prototype scale. The footing features five pressure sensors: one pore pressure transducer is integrated in the spudcan tip, and one pair of total and pore pressure transducers each are located on the top and bottom faces of the footing. Because this study focuses on the spudcan response, no attempt was made to model the trusswork leg of a jack-up. Instead, a solid aluminium cylinder was used. A load cell connecting the spudcan and leg with the actuator measured the axial footing loads during the test.

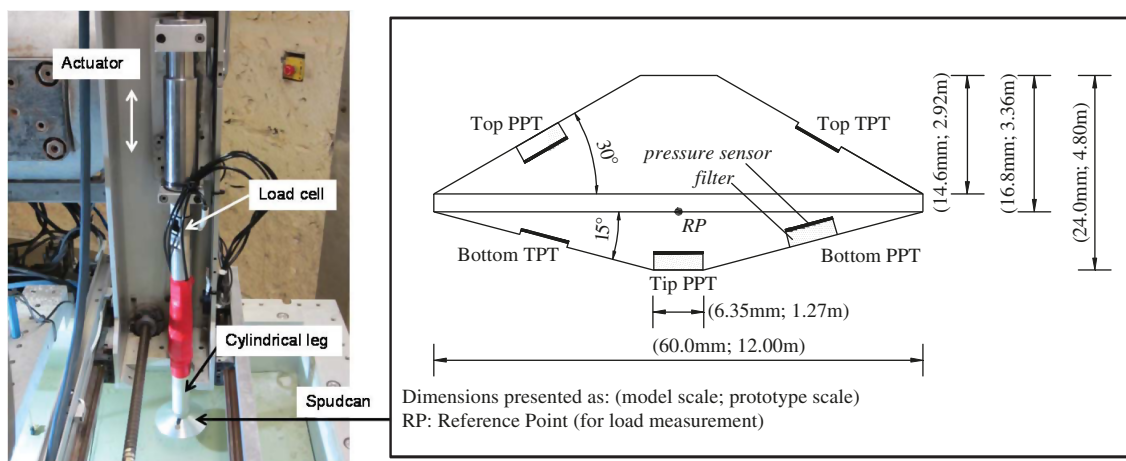


Fig. 2. Model spudcan and centrifuge setup

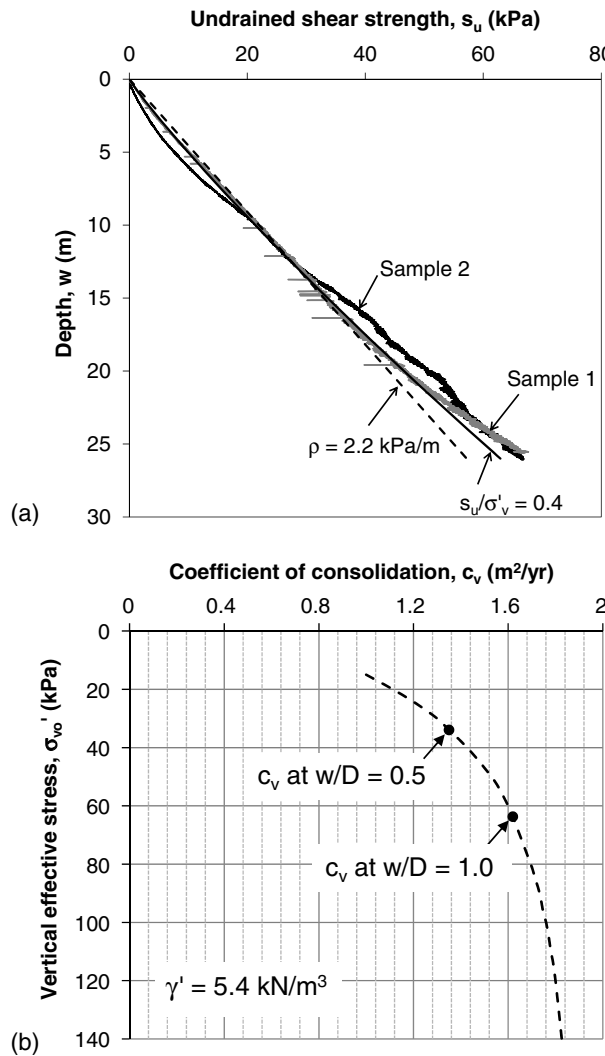


Fig. 3. (a) Undrained shear strength profiles obtained from miniature piezoball penetrometer testing; (b) coefficient of consolidation c_v obtained from Rowe cell test

Fig. 2 shows the model spudcan and the experimental setup. A half model spudcan of the same shape but a slightly smaller diameter of 50 mm was used in the PIV tests.

Sample Preparation

All new tests reported in this paper were performed on carbonate silty clay, which was recovered from the Laminaria field in the Timor Sea offshore Australia (Randolph et al. 1998a, b; Erbrich and Hefer 2002). For the first series of experiments, with full spudcan penetration, two samples were prepared using minimal added water and consolidated in flight in the beam centrifuge to create normally consolidated profiles. The water table was kept above the sample surface at all times. The samples were consolidated at 200 g for 5 days. Settlement of the sample surface during consolidation was measured using a linear displacement transducer. This confirmed negligible settlement rate after 5 days, and thus near full consolidation prior to commencement of the testing program. The final sample depth was ~150 mm, which allowed spudcan penetration to a depth of $2D$ (where D is the spudcan diameter) without adverse effects from the base of the strongbox (Bienen and Cassidy 2013). The samples for the drum centrifuge PIV tests were

Table 1. Overview of the Experiments

Consolidation Target depth	Test	Sample	Prototype time (s)					Average applied pressure (kPa)	$\Delta w/D$ due to consolidation	Peak w/D at peak	Reference N_c	Peak N_c / reference N_c	Postconsolidation	Extent of improved zone, $\Delta w_{ez}/D$	Severity of capacity reduction, K	
			Actual depth, w/D	0 years	0.5 years	5 years	64 years									
0.5D	SC-1 (PIV)	1	N/A	x	—	—	—	N/A	N/A	N/A	N/A	N/A	N/A	N/A	N/A	N/A
	SC-4	1	0.49	—	x	—	—	0.005	$6.4 \cdot 10^{-6}$	105.9	0.09	8.89	0.59	8.12	0.21	-2.08
	SC-6 (PIV)	1	0.50	—	—	x	—	0.052	$6.4 \cdot 10^{-5}$	115.3	0.13	11.58	0.66	7.99	1.45	-2.75
	S2-SC-6	2	0.49	—	—	x	—	0.623	$7.6 \cdot 10^{-4}$	85.5	0.14	13.51	0.65	8.04	1.68	-2.73
1.0D	SC-2 (PIV)	1	1.00	—	x	—	—	0.005	$2.9 \cdot 10^{-6}$	232.0	0.12	9.64	1.13	8.41	1.15	2.91
	SC-5 (PIV)	1	0.97	—	—	x	—	0.052	$2.9 \cdot 10^{-5}$	217.4	0.18	11.40	1.16	9.47	1.20	0.84
	SC-3 (PIV)	1	0.99	—	—	x (12 years)	—	0.746	$4.1 \cdot 10^{-4}$	220.1	0.22	16.45	1.27	8.46	1.94	-1.18
								(0.193)	$(1.1 \cdot 10^{-4})$							-4.24

Note: PIV refers to corresponding PIV test available.

^a N_c value of the reference case (SC-1) at the same penetration depth.

prepared in a similar fashion in custom-made strongboxes with a Perspex face.

The undrained soil shear strength s_u was evaluated using a miniature piezoball penetrometer, assuming a factor N_{Ball} of 10.5, as shown in Fig. 3(a). It is well represented by a linear fit with a gradient $\rho = 2.2 \text{ kPa/m}$ (2.9 kPa/m in the PIV tests). This gives a soil strength ratio $s_u/\sigma'_v = 0.4$ (0.5), considering a submerged unit weight of the soil $\gamma' = 5.4 \text{ kN/m}^3$. Episodes of penetrometer cycling were used to establish the sensitivity of the reconstituted soil samples, $S_t = 2.9$.

Fig. 3(b) provides the c_v profile obtained from Rowe cell testing, considering a submerged unit weight of the soil $\gamma' = 5.4 \text{ kN/m}^3$. The choice of soil allowed a wide range of degrees of consolidation to be investigated. The results are presented in terms of nondimensional consolidation time $T = c_v t / D^2$, which allows the findings to be viewed independent of the absolute time of consolidation, t .

Experimental Program and Procedure

The full spudcan penetration testing program comprised six tests with varying periods of consolidation at different penetration depths, as summarized in Table 1. In addition, one reference test was performed without interruption of the penetration process. The test procedure was as follows:

1. Undrained penetration under displacement control at a rate of 0.1 mm/s [with the normalized velocity $V = vD/c_v > 100$ indicating an undrained response as discussed by Finnie (1993), Chung et al. (2006), and Cassidy (2012)] to the depth targeted for the consolidation phase;
2. Consolidation under constant load of the magnitude just reached (this phase was omitted for the reference case); and
3. Further penetration (at a rate of 0.1 mm/s) to the final depth of $2D$.

The nondimensional consolidation times, T , investigated here ranged from 0.005 to 0.746, with consolidation taking place at $0.5D$ and $1.0D$ penetration for three tests each. Not only does this testing program cover a wide range of consolidation phases, but it also allows comparison of the results obtained in the carbonate silty

clay with those of similar tests performed in kaolin clay (Bienen and Cassidy 2013).

Corresponding PIV tests were performed for five of the six full spudcan tests, with an additional test at $1.0D$ penetration and $T = 0.01$, which allows further comparison with tests on kaolin clay (Stanier et al. 2014).

Experimental Results and Discussion

The experimental results are presented in nondimensional form unless stated otherwise. Table 1 summarizes the test details and results.

Increase in Bearing Resistance with Consolidation Time

Fig. 4 shows the measured penetration resistance in terms of the nondimensional bearing capacity factor, $N_c = V/(s_u A)$, where V is the vertical load on the spudcan, s_u is the in situ undrained shear strength of the soil as inferred from the fitted linear profile at that depth; and A is the largest plan area of the spudcan. {The choice of s_u for normalization is the reason the only test performed in Sample 2 has an apparently lower bearing capacity factor [Fig. 4(a)] initially.} The corresponding results from tests in kaolin clay (Bienen and Cassidy 2013) are included for comparison.

The bearing capacity factor quickly reaches an approximately constant value, indicating the transition to a localized mechanism with a stable cavity depth, or depression, at the soil surface. During consolidation, the bearing capacity factor decreases due to the normalization by the increasing undrained shear strength corresponding to the spudcan settlement under the constant load in this phase. Following consolidation, a sharp increase in bearing resistance is measured, which, after reaching a peak value, gradually reduces again. This general response follows the schematic shown in Fig. 1 and is similar to that observed in kaolin clay (Bienen and Cassidy 2013). However, there are significant differences as well.

The bearing capacity factor, N_c , is slightly lower in the carbonate silty clay than in the kaolin clay. The full spudcan test results

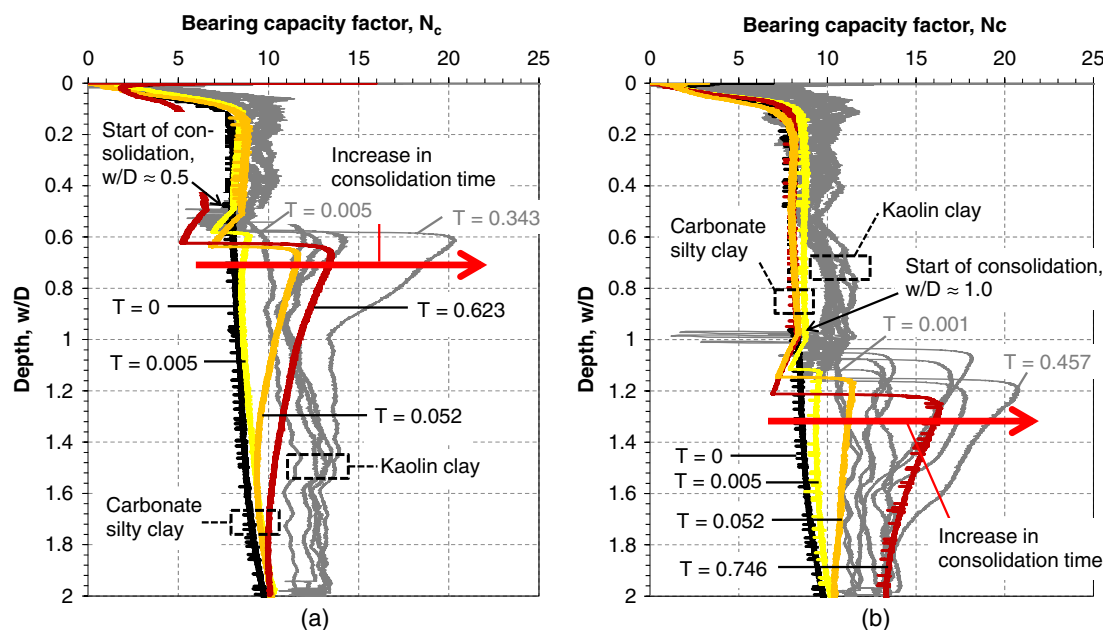


Fig. 4. Increase in bearing resistance with consolidation time at (a) $0.5D$; (b) $1.0D$ penetration

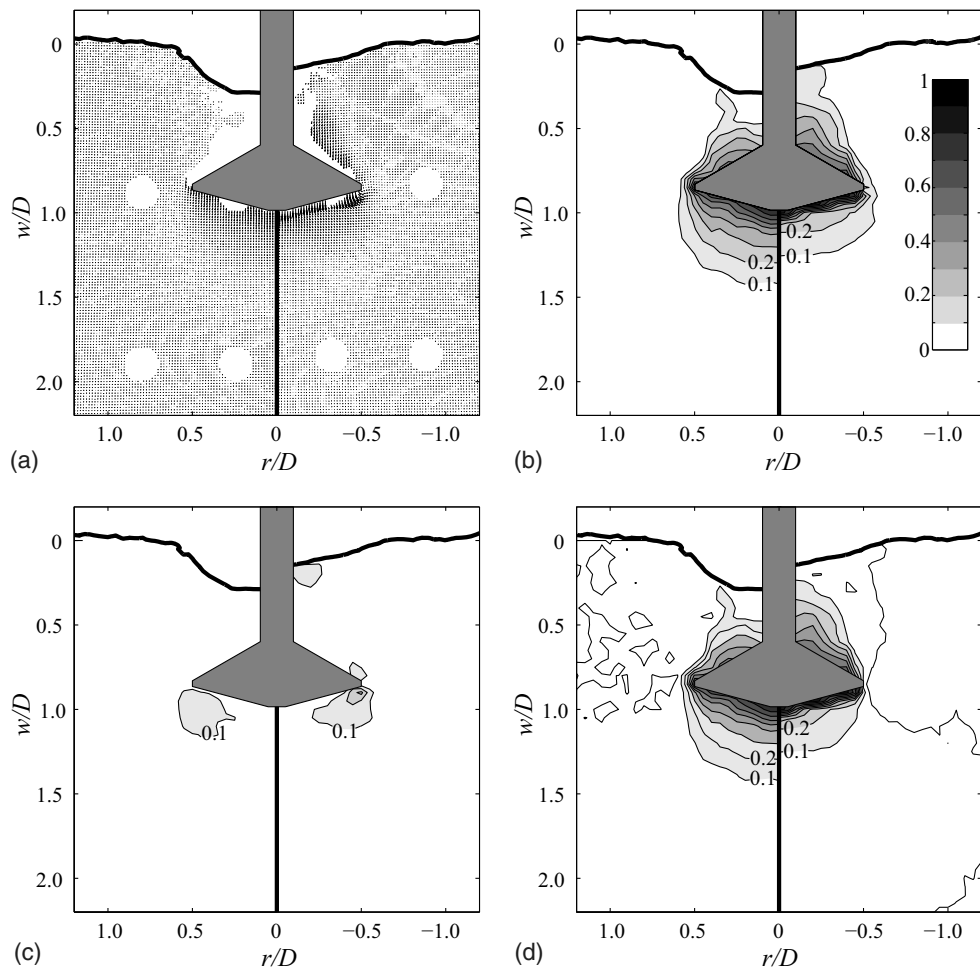


Fig. 5. Evidence of differences in mechanism between carbonate silty soil (left-hand side) compared to kaolin clay (right-hand side): (a) normalized vectorial velocities; (b) normalized resultant velocity contours v_r/v_f ; (c) normalized horizontal velocity contours v_h/v_f ; (d) normalized vertical velocity contours v_v/v_f

cannot provide sufficient insight to resolve the reasons for this difference, though the slight difference in spudcan shape between the model used in testing here and Bienen and Cassidy (2013) is unlikely to be responsible because the measurements of a spudcan penetrating into kaolin by Zhang et al. (2013, 2014) should then also be systematically lower than those by Barbosa-Cruz (2007), which is not the case.

The reasons for the lower bearing capacity factor in the carbonate silty clay are therefore explored using the results from corresponding PIV tests.

Fig. 5 reveals that the cause of the difference is that the spudcan penetration in the two soils is governed by different mechanisms, which is masked by expression of the response in terms of a bearing capacity factor, N_c . The differences are visible in Fig. 5(a), which shows the incremental displacement vectors, but becomes clearer when viewed in terms of contours of incremental displacement [Figs. 5(b–d)], where v_r , v_h , and v_v are the resultant, horizontal, and vertical velocities of the soil, normalized by the footing penetration velocity v_f . The relatively large extent of vertical displacements underneath the spudcan [Fig. 5(d)] with only limited horizontal displacements [Fig. 5(c)] in the carbonate silty clay is consistent with the high compressibility expected in the carbonate soil (as evidenced also in Rowe cell testing) and a plunging

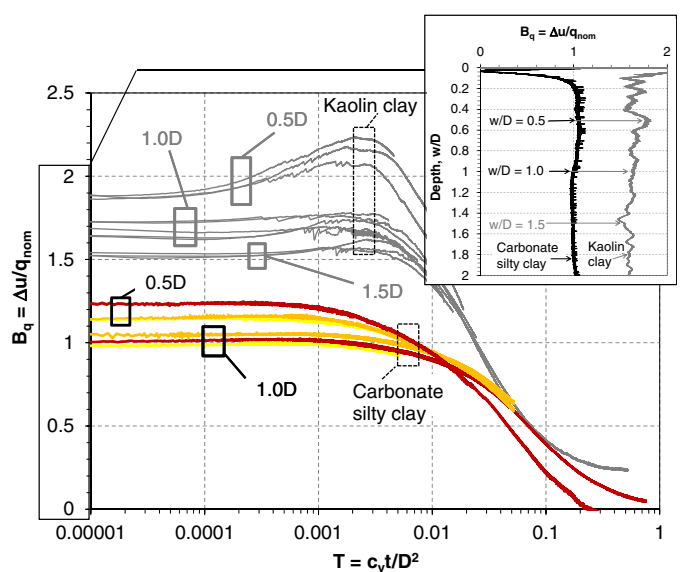


Fig. 6. Time history of excess pore pressure ratio, B_q , measured at the spudcan tip

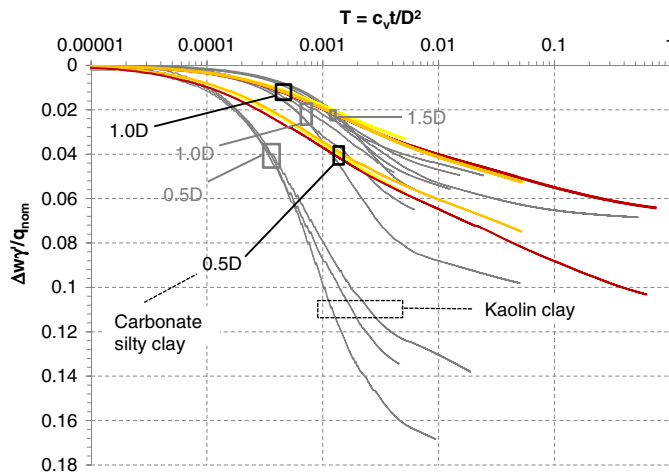


Fig. 7. Time history of dimensionless consolidation settlement, $\Delta w\gamma'/q_{\text{nom}}$

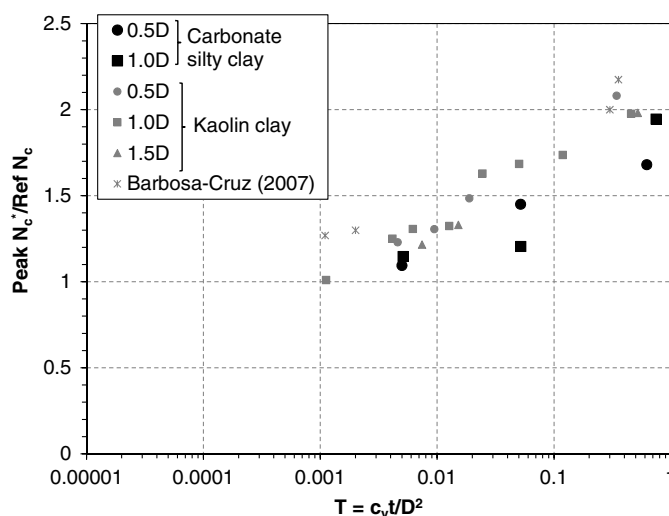


Fig. 8. Increase in bearing capacity factor, N_c^* , with normalized consolidation time

mechanism seen also in carbonate sand (Yamamoto et al. 2008; Dijkstra et al. 2013). Spudcan penetration into normally consolidated kaolin clay, on the other hand, quickly transitions from general shear to the localised flow-around mechanism seen in Fig. 5. When expressed in terms of the bearing capacity factor, the relatively larger contribution of the stronger soil below the spudcan that forms part of the mechanism in the carbonate silty clay is balanced by the lower contribution of the remoulded soil above the spudcan due to its higher sensitivity, such that the resulting value of N_c overall is similar or slightly less than in kaolin clay.

Undrained spudcan penetration into the carbonate silty clay generates less excess pore pressures than in the kaolin clay (Fig. 6 inset, measured at the spudcan tip). The differences in soil characteristics further influence the shape of the consolidation curves as shown in Fig. 6. In kaolin clay, the excess pore pressure at the spudcan tip in the early stages of consolidation increase before dissipating because the redistribution of stress concentrations and consolidation-induced settlement result in the generation of additional excess pore pressure that initially outweigh the dissipation of excess pore pressures generated during spudcan penetration. This Mandel-Cryer effect is less pronounced at deeper embedment where soil strength and confining stress are higher. In the carbonate silty clay where s_u increases more strongly with effective stress, the Mandel-Cryer effect was absent in all of the tests. The higher undrained shear strength gradient compared to the kaolin clay results in reduced settlement in the carbonate silty clay (Fig. 7).

The maximum bearing capacity factor postconsolidation compared with that of the reference case without consolidation at the corresponding penetration depth is broadly similar between the two soil types as shown in Fig. 8 (with the legend referring to the respective penetration depth prior to consolidation), though perhaps the data points representing the carbonate silty clay plot slightly lower than the corresponding points for the kaolin clay. In the tests involving consolidation, it is perhaps overly simplistic to refer to the bearing capacity factor, N_c , because both the undrained shear strength profile and the failure mechanism are changed [which for kaolin clay is discussed in Stanier et al. (2014)]. Therefore, N_c^* is a better representation of the bearing capacity factor that combines both these influences. This notation is adopted here.

Though the mechanism prior to consolidation differs between the two soil types, the general qualitative change following a

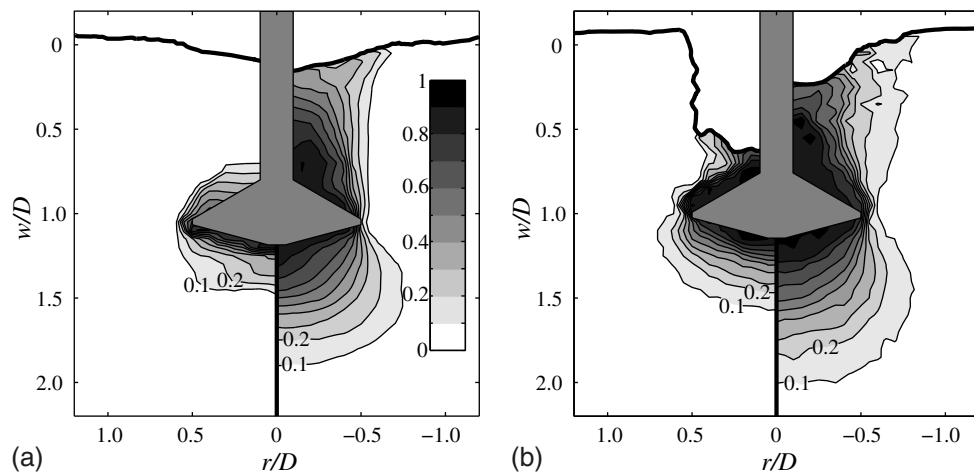


Fig. 9. Normalized resultant displacement contours: (a) kaolin clay; (b) carbonate silty clay, $T = 0$ (left-hand side), $T = 0.05$ (right-hand side)

significant period of consolidation is similar, as shown for $T = c_v t / D^2 = 0.05$ in Fig. 9.

The relative differences, therefore, remain similar: N_c was slightly lower in the carbonate silty clay as discussed previously. Immediately postconsolidation, the mechanism is significantly enlarged in both soils, giving rise to the considerable increase in peak N_c^* /reference N_c of 1.20 in the full spudcan test (1.34 in the PIV test) in the carbonate silty clay and 1.69 (1.66) in the kaolin,

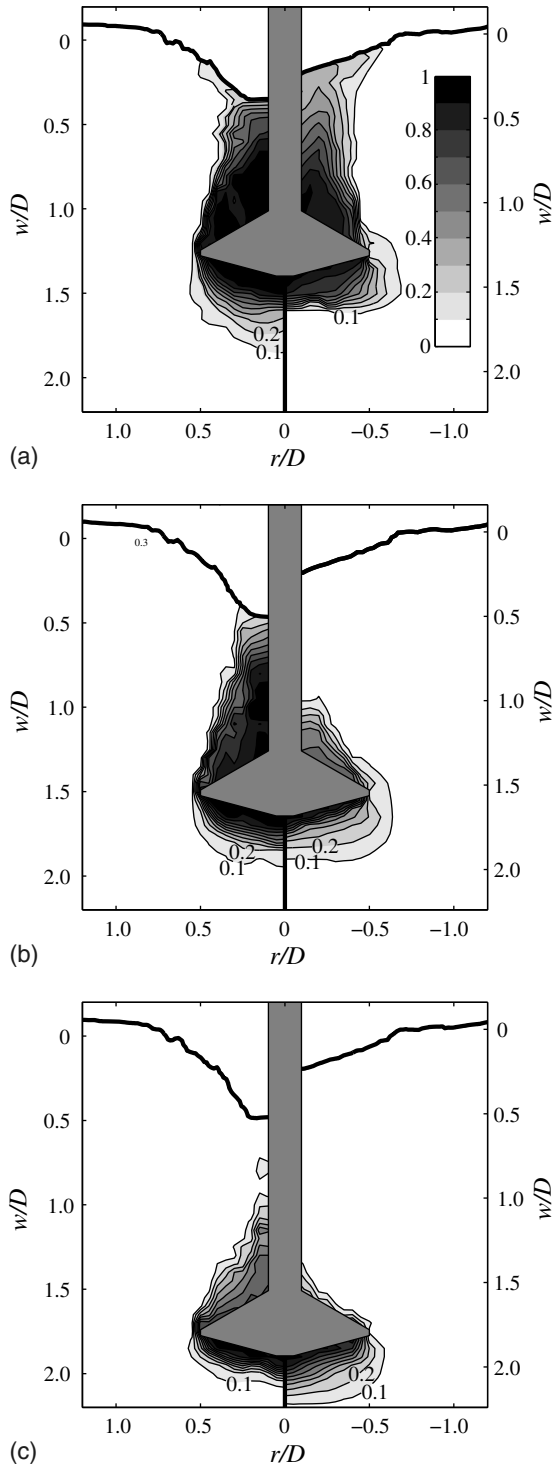


Fig. 10. Mechanism postpeak in terms of normalized resultant displacement contours v_r/v_f , after (a) $0.25D$, (b) $0.5D$, (c) $0.75D$, carbonate silty clay (left-hand side), kaolin clay (right-hand side)

respectively, for $T = 0.05$ (Fig. 8 shows that the difference is less for other periods of consolidation). In both soils, the extent of the mechanism increased significantly below the spudcan compared with the case without the effects of consolidation, as well as now extending to the soil surface, despite embedment of about $1D$.

Evolution of Load-Penetration Response Postconsolidation

The most striking difference in behavior between the two soil types is the shape of the load-penetration curve postpeak (Fig. 4). In the carbonate silty clay, N_c^* gradually reduces before gently curving around to rejoin the response of the reference case without consolidation. In kaolin, however, the postpeak reduction, especially for longer periods of consolidation, is much more pronounced and the curve does not merge with the reference case; it features continuously increased resistance.

While the mechanism governing the response in kaolin rapidly returns to localized flow around the footing [Fig. 10(b), after $0.5D$ of penetration postpeak], the behavior in the carbonate silty clay shows significant differences. After penetrating $0.25D$ postpeak, the normalized resultant displacement contours extend considerably further below the spudcan [Fig. 10(a)], and after $0.5D$ the mechanism still involves the soil column above the spudcan up to the soil surface [Fig. 10(b)]. Even though the behavior tends to a localized mechanism in the carbonate silty clay, this transition is not complete after $0.75D$ of penetration postpeak [Fig. 10(c)]. Throughout, the response in the carbonate silty clay is limited in its lateral extent, while a wider zone of soil is affected by the discontinuous spudcan penetration in kaolin.

The postpeak behavior can be described by the (negative) gradient of penetration resistance, K , that describes the overall reduction in N_c^* from its maximum until no further effect of consolidation is evident and the gradient of the penetration curve returns to be parallel to the reference case (Fig. 11, inset). Though peak N_c^* is readily identified, some uncertainty is attached to the determination of K because the effects of consolidation diminish and thus merging of the curves occurs gradually. This is evident in the scatter in Fig. 11.

As a general trend, though, K increases with increasing consolidation, as expected. However, the magnitude of this gradient is consistently and significantly lower in the carbonate silty clay

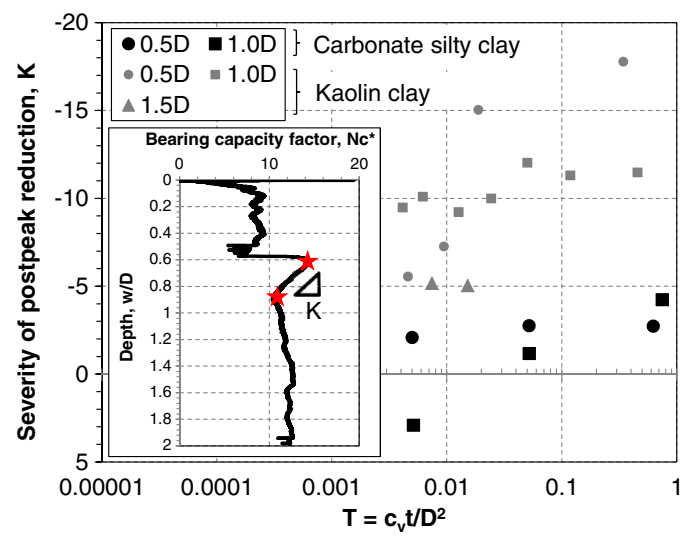


Fig. 11. Severity of capacity reduction K postpeak

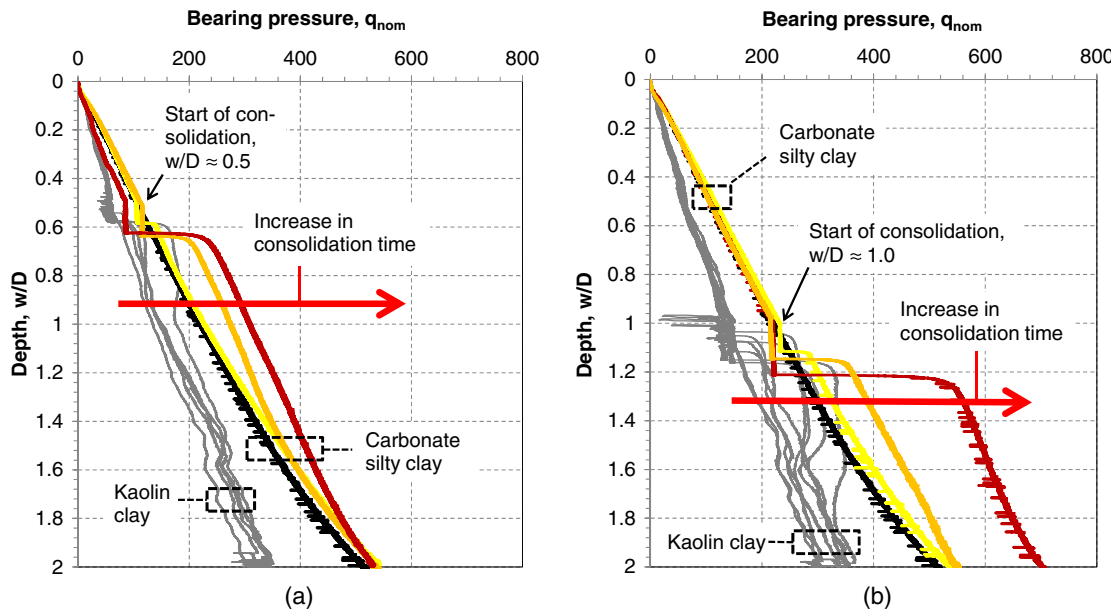


Fig. 12. Penetration resistance profiles with consolidation at (a) $0.5D$; (b) $1.0D$ penetration

compared with kaolin, and so is the increase with consolidation. This highlights the much gentler postpeak behavior of the former already seen in Fig. 4. The response is considerably more ductile, and the load-penetration curve postconsolidation rejoins that of the reference case [in kaolin the gradient became similar though the penetration resistance retained an offset to the curve without consolidation (Bienen and Cassidy 2013)].

While the response normalized by the undrained shear strength decreases postpeak, the penetration resistance does not (Fig. 12). Hence, consolidation does not introduce a man-made risk of uncontrolled rapid penetration or punch through in the carbonate silty clay (at least within the range of experimental conditions investigated) because the penetration resistance curve does not feature a peak or postpeak reduction. In contrast, the bearing pressure continuously increases following a sharp rise immediately postconsolidation. This is an important finding, which sets the effects of consolidation in the carbonate silty clay apart from those in kaolin, where the potential for punch through, or at least rapid leg run, is evident.

The gradient postpeak, of course, is influenced by the vertical distance between peak N_c^* and the return to the load-penetration curve that is unaffected by consolidation. This vertical distance is termed here the extent of the improved zone.

Because the dissipation of excess pore pressures progresses with time, thus allowing enhancement of effective stresses, the extent of the improved zone increases with the length of the consolidation period for both soils as expected (Fig. 13). However, the extent of the improved zone increased much more sharply with increasing T in the carbonate silty clay, such that two distinctly different trends emerge for the soils investigated (Fig. 13). While the peak response is described well in terms of the coefficient of consolidation, dissipation of excess pore pressure that eventually determines the extent of the improved zone is better described as a function of the permeability rather than including stiffness characteristics. Therefore, framing the information in Fig. 14 in terms of normalized permeability $k t/D$, where k is the permeability (from Rowe cell testing), t is the absolute consolidation time, and D is the maximum spudcan diameter, brings the data for both soils together as

illustrated in Fig. 14 (accepting the limited accuracy of permeability measurements).

The depth at which the installation is interrupted does not have a significant influence on the characteristics of the postconsolidation behavior: the data points representing consolidation at $0.5D$, $1.0D$, and $1.5D$ (the latter data available for kaolin only) all fall within a narrow band, with no specific trends with depth discernible for peak N_c^* , K , or the extent of the improved zone (Figs 8, 11, and 14).

Proposed Framework to Predict the Effect of Consolidation on the Load-Penetration Curve

Based on the findings from the centrifuge testing program, the following framework is suggested to predict the effect of consolidation on the load-penetration curve:

- Prior to consolidation, the load-penetration curve is estimated as $q_{\text{nom}} = V/A = N_c s_u$, where q_{nom} is the bearing pressure, V is

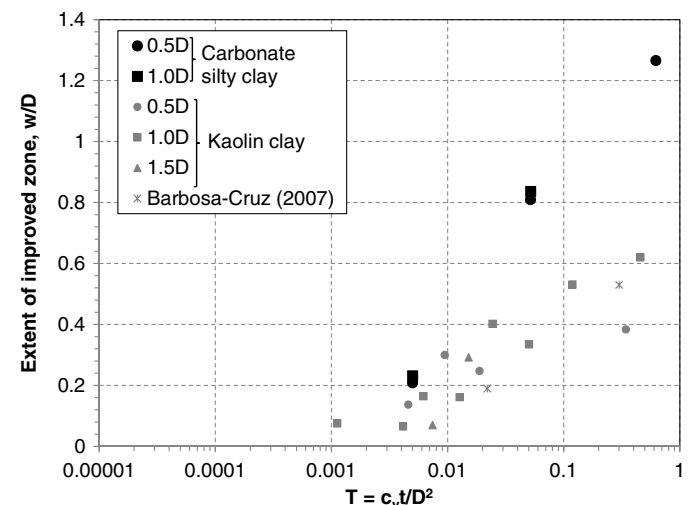


Fig. 13. Extent of improved zone with normalized consolidation time

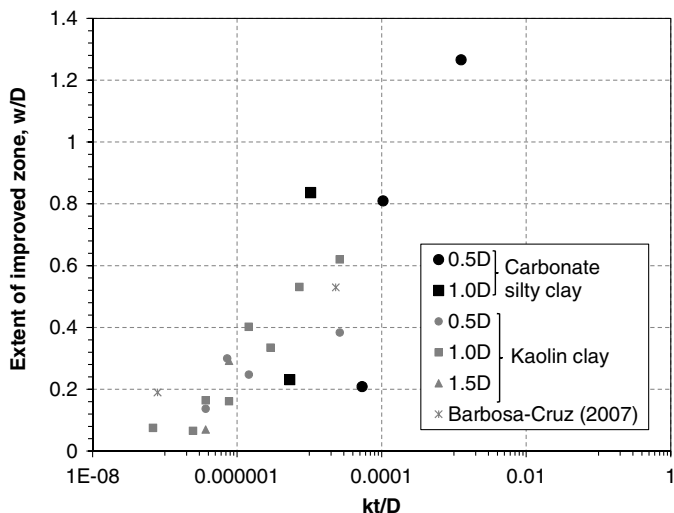


Fig. 14. Extent of improved zone with normalized permeability

the vertical load, A is the effective bearing area of the spudcan, and s_u is the undrained shear strength as determined from site investigation. The bearing capacity factor N_c has been established for spudcans in kaolin by Hossain and Randolph (2009) while Fig. 4 provides the values for the carbonate silty clay tested in this study. ISO (2012) provides detailed guidance on the prediction of load-penetration curves.

- During a pause in installation, additional settlement is accumulated, which can be estimated according to Fig. 15. At the time of testing the level of sophistication of load control was higher in the beam centrifuge tests on the carbonate silty clay, which is the cause of the scatter in the data obtained on kaolin clay in the drum centrifuge. Though it is acknowledged that the settlement depends on the pressure applied during consolidation (relative to the available bearing capacity at that depth), there is insufficient data available at present to include this secondary effect. Ongoing research, including large deformation numerical analyses with coupled pore fluid stress response, will allow further refinement.
- On recommencement of penetration, the response features high stiffness. The maximum bearing pressure q_{peak} can be estimated

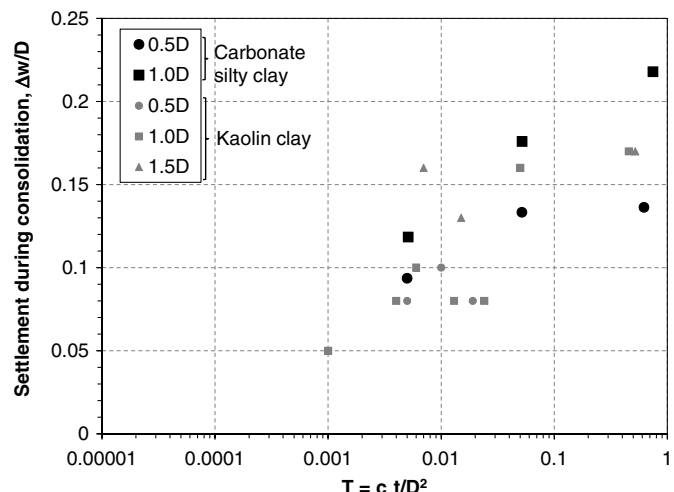


Fig. 15. Normalized consolidation settlement with normalized consolidation time

based on the original undrained shear strength at that depth s_u , the bearing capacity factor N_c expected without consolidation, and the enhancement factor peak $N_c^*/\text{reference } N_c$ (Fig. 8).

- The extent of the improved zone, depending on the soil permeability, can be estimated from Fig. 14. In carbonate silty soil, this marks the transition to a load-penetration curve unaffected by consolidation, whereas in kaolin the effective bearing capacity factor N_c^* remains enhanced by approximately 20% compared with the reference case even after 0.5–1.0D of further penetration (Stanier et al. 2014).

Prediction of the effects of consolidation on the load-penetration curve requires knowledge of the coefficient of consolidation, c_v , and the permeability of the soil, k . It is therefore recommended to perform in situ testing with a penetrometer that is equipped to measure pore pressure response or to include odometer or Rowe cell testing on undisturbed (if possible) soil specimen in the site investigation work scope.

The effects of consolidation may be detrimental (e.g., when causing punch through or rapid leg run, especially if this was not predicted) or advantageous and thus actively sought. The latter may be the case if consolidation offered adequate bearing capacity at much shallower penetration, particularly in deep water where available leg length may become critical. However, reliability of this enhanced capacity both under the general low-level cyclic loading of the ocean environment and under storm loading must be ensured. Therefore, investigation of the reliability of the postconsolidation capacity under cyclic loading will be addressed in further research.

The results and discussions in this paper are not only relevant to penetrating footings but also shed light on the state of the soil around a jack-up spudcan immediately prior to its extraction for instance, a problem that has been investigated by Purwana et al. (2005), Bienen et al. (2009), and Gaudin et al. (2011a). The inability to predict s_u postconsolidation has been a major stumbling block in developing a predictive method such as attempted by Purwana et al. (2009).

Concluding Remarks

The effects of a period of consolidation interrupting footing penetration in carbonate silty clay have been investigated in a series of centrifuge experiments, complemented by visualization experiments, also carried out in a geotechnical centrifuge. Parallels to an earlier study on kaolin clay allowed differentiation of the general features of the response against differences in detail when comparing the two soil types.

This paper offers graphs useful for the estimation of peak resistance postconsolidation based on the experimental results and proposes a framework to predict the effect of consolidation on the load-penetration curve of the footing.

Acknowledgments

The first author is the recipient of an Australian Research Council (ARC) Postdoctoral Fellowship (DP110101603) and the third author is the recipient of an ARC Laureate Fellowship (FL130100059). This work forms part of the activities of the Centre for Offshore Foundation Systems (COFS), currently supported as a node of the ARC Centre of Excellence for Geotechnical Science and Engineering and as a Centre of Excellence by the Lloyd's Register Foundation. Lloyd's Register Foundation invests in science, engineering, and technology for public benefit, worldwide. This support is gratefully acknowledged.

References

- Barbosa-Cruz, E. R. (2007). "Partial consolidation and breakthrough of shallow foundations in soft soil." Ph.D. thesis, Univ. of Western Australia, Perth, Australia.
- Bienen, B., and Cassidy, M. J. (2013). "Set-up and resulting punch-through risk of jack-up spudcans during installation." *J. Geotech. Geoenviron. Eng.*, **10.1061/(ASCE)GT.1943-5606.0000943**, 2048–2059.
- Bienen, B., Gaudin, C., and Cassidy, M. J. (2009). "The influence of pull-out load on the efficiency of jetting during spudcan extraction." *Appl. Ocean Res.*, **31**(3), 202–211.
- Brennan, R., et al. (2006). "Installing jackups in punch-through sensitive clays." *Proc., Offshore Technology Conf. (OTC)*, Society of Petroleum Engineers, Richardson, TX.
- Cassidy, M. J. (2012). "Experimental observations of the penetration of spudcan footings in silt." *Géotechnique*, **62**(8), 727–732.
- Chung, S. F., Randolph, M. F., and Schneider, J. A. (2006). "Effect of penetration rate on penetration resistance in clay." *J. Geotech. Geoenviron. Eng.*, **10.1061/(ASCE)1090-0241(2006)132:9(1188)**, 1188–1196.
- Craig, W. H., and Chua, K. (1990). "Deep penetration of spudcan foundations on sand and clay." *Géotechnique*, **40**(4), 541–556.
- Dijkstra, J., Gaudin, C., and White, D. J. (2013). "Comparison of failure modes below footings on carbonate and silica sands." *Int. J. Phys. Modell. Geotech.*, **13**(1), 1–12.
- Erbrich, C., and Hefer, P. (2002). "Installation of the Laminaria suction piles—A case history." *Offshore Technology Conf.*, Society of Petroleum Engineers, Richardson, TX.
- Erbrich, C. T. (2005). "Australian frontiers—Spudcans on the edge." *Proc., Int. Symp. on Frontiers in Offshore Geotechnics (ISFOG)*, Taylor & Francis, London, 49–74.
- Finnie, I. M. S. (1993). "Performance of shallow foundations in calcareous soil." Ph.D. thesis, Univ. of Western Australia, Perth, Australia.
- Garnier, J., et al. (2007). "Catalogue of scaling laws and similitude questions in centrifuge modelling." *Int. J. Phys. Modell. Geotech.*, **7**(3), 1–24.
- Gaudin, C., Bienen, B., and Cassidy, M. J. (2011a). "Investigation of the potential of bottom water jetting to ease spudcan extraction in soft clay." *Géotechnique*, **61**(12), 1043–1054.
- Gaudin, C., Cassidy, M. J., Bienen, B., and Hossain, M. S. (2011b). "Recent contributions of geotechnical centrifuge modelling to the understanding of jack-up spudcan behaviour." *Ocean Eng.*, **38**(7), 900–914.
- Hossain, M. S., and Randolph, M. F. (2009). "New mechanism-based design approach for spudcan foundations on single layer clay." *J. Geotech. Geoenviron. Eng.*, **10.1061/(ASCE)GT.1943-5606.0000054**, 1264–1274.
- Hossain, M. S., and Randolph, M. F. (2010a). "Deep-penetrating spudcan foundations on layered clays: Centrifuge tests." *Géotechnique*, **60**(3), 157–170.
- Hossain, M. S., and Randolph, M. F. (2010b). "Deep-penetrating spudcan foundations on layered clays: Numerical analysis." *Géotechnique*, **60**(3), 171–184.
- Hu, P., Stanier, S., Cassidy, M. J., and Wang, D. (2014). "Predicting the peak resistance of a spudcan penetrating sand overlying clay." *J. Geotech. Geoenviron. Eng.*, **140**(2), 04013009.
- Hunt, R. (2008). "Achieving operational excellence for jack-up rig deployments—how shall we get there?" *Proc., 2nd Jack-Up Asia Conf. and Exhibition*, PetroMin, Singapore.
- ISO (International Organization for Standardization). (2012). "Petroleum and natural gas industries—Site-specific assessment of mobile offshore units—Part 1: Jack-ups." Geneva.
- Jack, R. L., Hoyle, M. J. R., Smith, N. P., and Hunt, R. J. (2013). "Jack-up accident statistics—A further update." *Proc., 14th Int. Conf. on the Jack-Up Platform: Design, Design, Construction and Operation*, City Univ., London.
- Lee, K. K., Cassidy, M. J., and Randolph, M. F. (2013a). "Bearing capacity on sand overlying clay soils: Experimental and finite-element investigation of potential punch-through failure." *Géotechnique*, **63**(15), 1271–1284.
- Lee, K. K., Randolph, M. F., and Cassidy, M. J. (2013b). "Bearing capacity on sand overlying clay soils: A simplified conceptual model." *Géotechnique*, **63**(15), 1285–1297.
- Osborne, J. J., Pelley, D., Nelson, C., and Hunt, R. (2006). "Unpredicted jack-up foundation performance." *Proc., Jack-Up Asia Conf. and Exhibition*, PetroMin, Singapore.
- Purwana, O. A., Leung, C. F., Chow, Y. K., and Foo, K. S. (2005). "Influence of base suction on extraction of jack-up spudcans." *Géotechnique*, **55**(10), 741–753.
- Purwana, O. A., Quah, M., Foo, K. S., Nowak, S. and Handijaja, P. (2009). "Leg extraction/pullout resistance: Theoretical and practical perspectives." *Proc., 12th Int. Conf. on the Jack-Up Platform: Design, Construction and Operation*, City Univ., London.
- Qiu, G., and Grabe, J. (2012). "Numerical investigation of bearing capacity due to spudcan penetration in sand overlying clay." *Can. Geotech. J.*, **49**(12), 1393–1407.
- Randolph, M. F., Hefer, P. A., Geise, J. M., and Watson, P. G. (1998a). "Improved seabed strength profiling using T-bar penetrometer." *Proc., Int. Conf. on Offshore Site Investigation and Foundation Behaviour—'New Frontiers'*, Society for Underwater Technology, London, 221–235.
- Randolph, M. F., Jewell, R. J., Stone, K. J. L., and Brown, T. A. (1991). "Establishing a new centrifuge facility." *Proc., Int. Conf. on Centrifuge Modelling, Centrifuge 91*, 3–9.
- Randolph, M. F., O'Neill, M. P., Stewart, D. P., and Erbrich, C. (1998b). "Performance of suction anchors in fine-grained calcareous soils." *Offshore Technology Conf.*, Society of Petroleum Engineers, Richardson, TX.
- Stanier, S., Ragni, R., Bienen, B., and Cassidy, M. J. (2014). "Observing the effects of sustained loading on spudcan footings in clay." *Géotechnique*, **64**(11), 918–926.
- Stanier, S. A., and White, D. J. (2013). "An improved image based deformation measurement system for the centrifuge environment." *Geotech. Test. J.*, **36**(6), 915–927.
- Stewart, D. P., Boyle, R. S., and Randolph, M. F. (1998). "Experience with a new drum centrifuge." *Proc., Int. Conf. Centrifuge 98*, 35–40.
- Teh, K. L., Leung, C. F., Chow, Y. K., and Cassidy, M. J. (2010). "Centrifuge model study of spudcan penetration in sand overlying clay." *Géotechnique*, **60**(11), 825–842.
- Yamamoto, N., Randolph, M. F., and Einav, I. (2008). "Simple formulas for the response of shallow foundations on compressible sands." *Int. J. Geomech.*, **10.1061/(ASCE)1532-3641(2008)8:4(230)**, 230–239.
- Yu, L., Hu, Y., Liu, A., Randolph, M. F., and Kong, X. (2012). "Numerical study of spudcan penetration in loose sand overlying clay." *Comput. Geotech.*, **46**, 1–12.
- Zhang, Y., Bienen, B., and Cassidy, M. J. (2013). "Development of a combined VHM loading apparatus for a geotechnical drum centrifuge." *Int. J. Phys. Modell. Geotech.*, **13**(1), 13–30.
- Zhang, Y., Cassidy, M. J., and Bienen, B. (2014). "A plasticity model for spudcan foundations in soft clay." *Can. Geotech. J.*, **51**(6), 629–646.